BULLETIN OF THE POLISH ACADEMY OF SCIENCES
TECHNICAL SCIENCES, Vol. 61, No. 4, 2013
DOI: 10.2478/bpasts-2013-0083

Dedicated to Professor M.P. Kaźmierkowski
on the occasion of his 70th birthday

Modern Direct Torque and Flux Control methods of an induction machine supplied by three-level inverter

A. SIKORSKI, K. KULIKOWSKI*, and M. KORZENIEWSKI

Department of Power Electronics and Electric Drivers, Bialystok University of Technology, 45D Wiejska St., 15-351 Bialystok, Poland

Abstract. This paper describes two modern direct torque and flux control methods of an induction machine supplied by a three-level inverter. Additionally, it presents a comparison of the methods both in static and dynamic states. The methods, in a specific way, make use of an increased number of active vectors of the three-level inverter in order to improve control quality and reduce switching frequency. The two methods modify the DTC method by using its advantages and eliminating, at the same time its drawbacks.

In static states the comparison was based on the results of investigations performed for two different load values and three set values of angular speed, whereas in dynamic states the comparison was focused on the behavior of the machine at startup.

The results of the investigations have shown that both methods give very good performance. They are characterized by both sinusoidal shape of flux and low current deformations even at low angular speeds i.e. less than 10% of the nominal value. The presented methods also allow to generate nominal flux for set zero angular speed in order to achieve excitation of the induction machine. The switching frequencies for both methods are very similar in almost the whole range of control but the methods have shown some differences in control quality, particularly for higher torque values.

Key words: asynchronous machine, DC/AC inverter, DTC, flux and torque control, 3-level DC/AC inverter.

1. Introduction

A DC/AC inverter constitutes the main part of AC drives. The most commonly used inverter configuration is a 6T+6D two-level structure. This type of inverters is used especially for systems supplied by low level voltages (3×230 V). A competitive structure for a two-level inverter is its three-level arrangement, particularly for systems supplied by higher level voltages. A three-level structure makes it possible to use transistors with twice lower nominal voltage in comparison with two-level inverters.

Three-level inverters consist of twice more transistors [1], but if we consider the fact that each switching occurs at a twice lower voltage, then we can state that the efficiency of both structures is similar for comparable switching frequencies. It should be noticed here that if an inverter is controlled by a method dedicated for a three-level structure, it is possible to achieve lower switching frequency (better efficiency) and similar control quality or alternatively, better control quality and similar switching frequency (similar efficiency) in comparison with a two-level inverter. Depending on the user's aims, either better control quality or better efficiency can be chosen.

Two-level inverters have only 6 active and 2 zero vectors available, whereas three-level structures offer 24 active and 3 zero vectors. Therefore, three-level inverters offer greater possibilities of control.

The standard DTC method [2] is dedicated for two-level inverters and has some disadvantages that are manifested especially at low angular speeds. There have been a number of publications devoted to the improvement of the standard DTC method [3–6]. Yet another approach to the improvement of the classical conception of the nonlinear (hysteresis) torque and flux controllers is an introduction of additional modulation algorithms at the sampling time T_p [7, 8]. For this purpose additional triangular signals modulating the torque and flux errors are used to decrease pulsations simultaneously increasing inverter switching frequency. One of these methods consists in the use of adequate torque and flux controller structures, i.e. using linear controllers that, in the final stage, take advantage of space voltage modulation. These algorithms are called DTC-SVM [9, 10]. Despite the fact that the used torque and flux PI controllers have a longer response time to the torque step changes, the complex controller systems [11] bring their properties closer to the DTC method which applies the nonlinear controllers. A better way of solving DTC-ST problems is offered by multi-level converters in which a higher number of voltage vectors enable realization of different control algorithms [12].

In the case when at the end of the control structure there is a pulse width modulation (PWM, SVM), control methods of three-level inverters are basically adopted from two-level solutions. However, the three-level structure of a DC/AC inverter offers new opportunities for nonlinear control methods, e.g. for DTC and its modifications, as well as for predictive control methods.

This paper considers two control methods: the DTC-sδ-12s and the DTFC-3L-3Am. Both of them are based on the DTC method and eliminate its basic disadvantages i.e. the hexagonal shape of flux and deformed current at low angular speeds (less than 10% the nominal value) as well as problems

*e-mail: k.kulikowski@pb.edu.pl

during startup (caused by inability to generate nominal flux for set zero angular speed). Disadvantages of the standard DTC method are mainly caused by a stator voltage vector deviation from the q-axis of the dq reference frame. This deviation significantly increases at low angular speeds and in effects decrease of control quality which is caused by incorrect selection of inverter voltage vectors. Both the DTC-sδ-12s and the DTFC-3L-3Am methods calculate this deviation called the δ angle that is included in the control system in order to increase the accuracy of control at low angular speeds. The proposed methods first calculate a specific error vector from torque and flux errors and next, using the specific error vector, choose which inverter voltage vector should be used in order to decrease the errors of controlled values. Apart from the calculation procedure of a specific error vector both methods differ in the way they use the calculated error vector. A choice of the inverter voltage vector in the DTC-sδ-12s method depends on the values of error vector components independently in d and q axes, but in the DTFC-3L-3Am this decision depends on the angle of the error vector.

Since the results of the investigations have shown that both methods are characterized by similar low values of switching frequencies and almost ideal sinusoidal shape of flux, their comparison focused mainly on the accuracy of moment control and current distortions.

2. Mathematical model of inverter

In the three-level structure of an inverter (Fig. 1) one of three electrical potentials ($+U_{DC}$, 0 or $-U_{DC}$) may appear at each of phase outputs. Owing to the choice of three possible states at each of three independent outputs, the output voltages of the inverter can be determined in $3^3 = 27$ valid combinations.

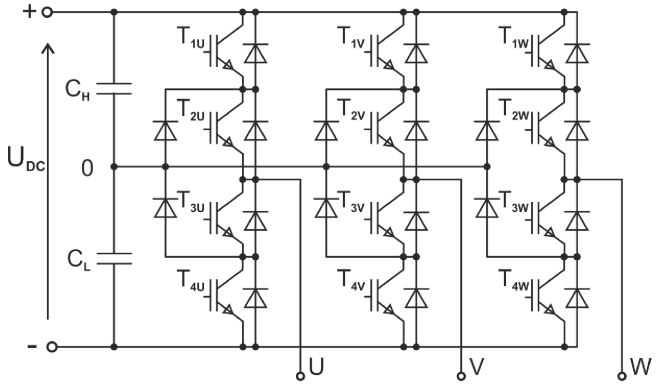

Fig. 1. Schematic diagram of the three-level inverter power circuit

$$\mathbf{U}_d[n] = \begin{cases} \frac{2}{3}U_{dc} \cdot e^{j(n-21)\frac{\pi}{3}}, \text{ for } n = \{21, 22..., 26\} \\ \frac{\sqrt{3}}{3}U_{dc} \cdot e^{j(n-15)\frac{\pi}{3}}, \text{ for } n = \{15, 16..., 20\} \\ \frac{1}{3}U_{dc} \cdot e^{j(n-3)\frac{\pi}{3}}, for n = \{3, 4, ..., 14\} \\ \text{“0”}, \text{ for } n = \{0, 1, 2\} \end{cases} \quad (1)$$

where $U_d[n]$ – inverter voltage vector, U_{dc} – DC link voltage, n – vector number (Fig. 2), “0” – zero vector.

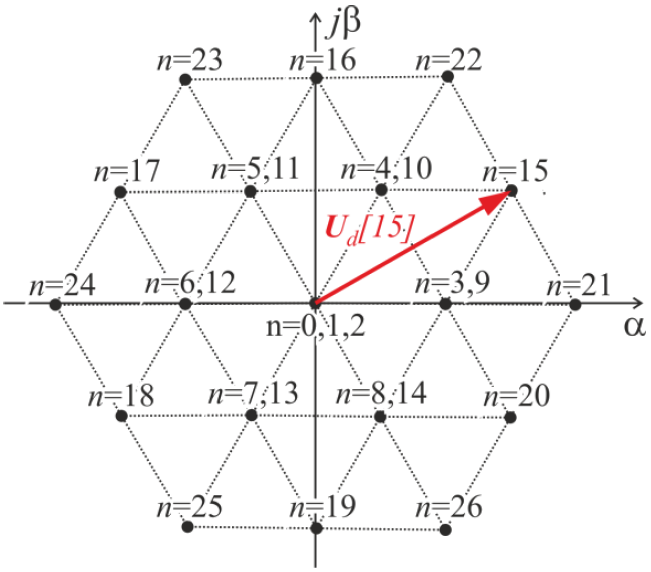

Fig. 2. Graphic representation of the inverter voltage vectors in the $\alpha\beta$ reference frame for three-level inverter

The relationships (1) [4] describe the output voltage vectors of the inverter in the $\alpha\beta$ stationary reference frame (Fig. 2) with respect to the three-level inverter configuration (Fig. 1).

3. Mathematical model of an induction machine supplied by inverter

An induction motor supplied by an inverter (Fig. 3) in the dq rotating reference frame can be described by the following formulas (2) and (2a) [4].

$$\mathbf{U}_d^{[}n] \cdot e^{-j\omega_s} = R_s\mathbf{I}_s + j\omega_s L_{\sigma s}\mathbf{I}_s + L_{\sigma s}\frac{d}{dt}\mathbf{I}_s + j\mathbf{E}, \quad (2)$$

$$\mathbf{U}_s^* = |\mathbf{U}_s^*| \cdot e^{\varphi \mathbf{U}_s^*} = R_s\mathbf{I}_s + j\omega_s L_{\sigma s}\mathbf{I}_s + j\mathbf{E}, \quad (2a)$$

where U_s^* – stator voltage vector in the dq reference frame, I_s – stator current vector, E – vector of electromotive force, ω_s – angular speed of stator flux vector, R_s – stator resistance, $L_{\sigma s}$ – leakage inductance of windings.

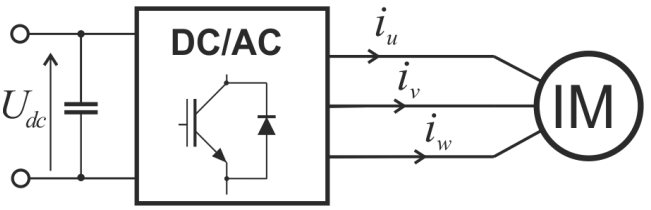

Fig. 3. Schematic diagram of an induction machine supplied by an inverter

Dependence (3) is achieved by the transformation of (2). The obtained voltage vector (Fig. 4a) is proportional to the

vector of stator current derivative (4) (Fig. 4b) that determines both the direction and speed of current changes.

$$\mathbf{D}_i[n] = \frac{d}{dt}\mathbf{I}_s = \frac{1}{L_{\sigma s}}(-(R_s\mathbf{I}_s + j\omega_s L_{\sigma s}\mathbf{I}_s + j\mathbf{E}) + \mathbf{U}_d^{[}n] \cdot e^{-j\omega_s}), \tag{3}$$

$$\mathbf{D}_u[n] = -\mathbf{U}_s^* + \mathbf{U}_d[n] \cdot e^{-j\omega_s}, \tag{3a}$$

$$\mathbf{D}_i[n] = \frac{1}{L_{\sigma s}}\mathbf{D}_u[n]. \tag{4}$$

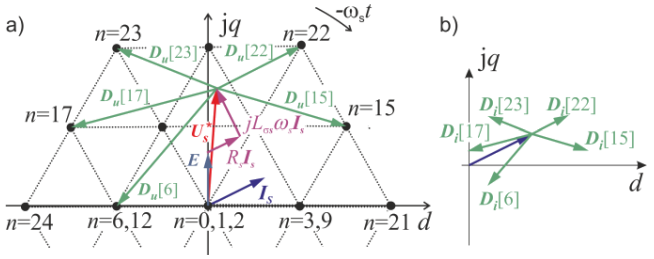

Fig. 4. Several examples of the voltage vectors proportional to the current derivative vectors $D_u[n]$ (a), and the corresponding current derivative vectors D_i $[n]$ (b)

In order to analyze the influence of current derivative vectors on torque and flux changes, the errors of flux and torque should be first converted to the current scale (Fig. 12) and then they may be treated as current vector components (5) [4].

$$\varepsilon^{=}_{i\Psi T}\varepsilon_{i\Psi} + j\varepsilon_{iT} = c_\Psi \cdot \varepsilon_\Psi + jc_T \cdot \varepsilon_T, \tag{5}$$

$$c_\Psi = \frac{i_{sdN}}{\Psi_{sN}} = \frac{1}{L_m}, \tag{5a}$$

$$c_T = \frac{i_{sqN}}{T_N} \cong \frac{2\omega_{sN}}{3p_b U_N\sqrt{2}} \tag{5b}$$

where ε_Ψ, ε_T – flux and torque errors, Ψ_{sN} – nominal value of flux, c_Ψ, c_T – current scale factors with respect to flux and torque, Ψ_{sN} – nominal value of flux, i_{sqN}, i_{sdN} – nominal values of stator current vector components, T_N – nominal value of torque, ω_{sN} – nominal value of synchronous angular speed, p_b – number of magnetic pole pair, U_n – nominal value of stator voltage.

4. Description of control methods

4.1. DTC-sδ-12s method. In the standard DTC method the area of inverter output voltage vectors is divided into six sectors, 60 degrees each, as shown in Fig. 5a. In order to make a full use of the advantages of three-level inverters in the DTC-sδ-12s method, the area of inverter output voltage vectors is divided into twelve sectors, 30 degrees each, in the way shown in Fig. 5b. Moreover, the standard DTC method is based on the assumption that the U_s^* stator voltage vector is shifted by 90 degrees with respect to the flux vector Ψ_s [2]. This assumption is correct only for near nominal angular speeds [4], when the angle of the U_s^* stator voltage vector is close to 90 degrees (Fig. 6a). At low angular speeds (Fig. 6b) the difference between the assumed and real angle of the U_s^* vector increases causing faulty operation of the standard DTC method [4].

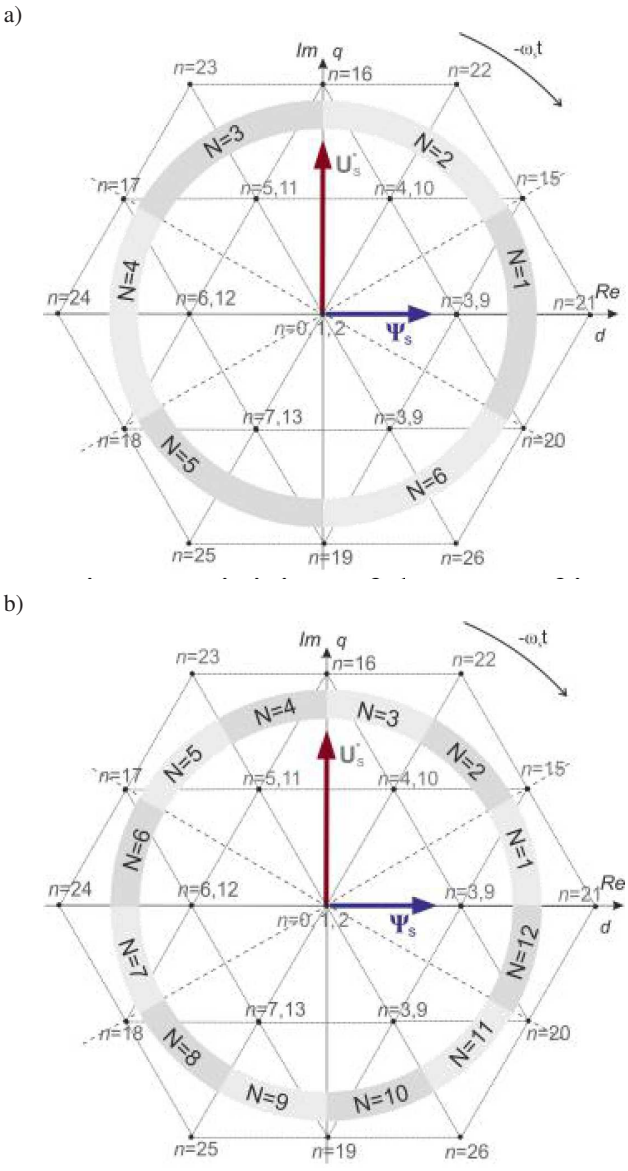

Fig. 5. Division of the area of inverter output voltage vectors into 6 (a) and 12 (b) sectors for three-level inverter

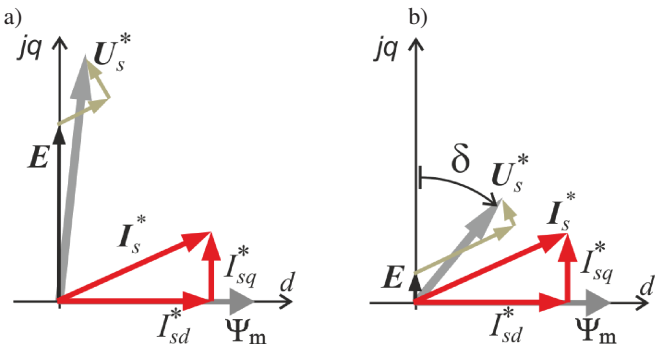

Fig. 6. Vector diagram of U_s^* stator voltage vector at near nominal (a) and low (b) rotor angular speeds

Table 1
Vector selection table for DTC-sδ-12s method

d_Ψ	d_T	$N=1$	$N=2$	$N=3$	$N=4$	$N=5$	$N=6$	$N=7$	$N=8$	$N=9$	$N=10$	$N=11$	$N=12$
1	2	$\boldsymbol{U}_d$ [16]	$\boldsymbol{U}_d$ [23]	$\boldsymbol{U}_d$ [17]	$\boldsymbol{U}_d$ [24]	$\boldsymbol{U}_d$ [18]	$\boldsymbol{U}_d$ [25]	$\boldsymbol{U}_d$ [19]	$\boldsymbol{U}_d$ [26]	$\boldsymbol{U}_d$ [20]	$\boldsymbol{U}_d$ [21]	$\boldsymbol{U}_d$ [15]	$\boldsymbol{U}_d$ [22]
	1	$\boldsymbol{U}_d$ [4]	$\boldsymbol{U}_d$ [11]	$\boldsymbol{U}_d$ [5]	$\boldsymbol{U}_d$ [12]	$\boldsymbol{U}_d$ [6]	$\boldsymbol{U}_d$ [13]	$\boldsymbol{U}_d$ [7]	$\boldsymbol{U}_d$ [14]	$\boldsymbol{U}_d$ [8]	$\boldsymbol{U}_d$ [9]	$\boldsymbol{U}_d$ [3]	$\boldsymbol{U}_d$ [10]
	0	$\boldsymbol{U}_d$ [1]	$\boldsymbol{U}_d$ [1]	$\boldsymbol{U}_d$ [0]	$\boldsymbol{U}_d$ [2]	$\boldsymbol{U}_d$ [1]	$\boldsymbol{U}_d$ [1]	$\boldsymbol{U}_d$ [0]	$\boldsymbol{U}_d$ [2]	$\boldsymbol{U}_d$ [1]	$\boldsymbol{U}_d$ [1]	$\boldsymbol{U}_d$ [0]	$\boldsymbol{U}_d$ [2]
	−1	$\boldsymbol{U}_d$ [8]	$\boldsymbol{U}_d$ [9]	$\boldsymbol{U}_d$ [3]	$\boldsymbol{U}_d$ [10]	$\boldsymbol{U}_d$ [4]	$\boldsymbol{U}_d$ [11]	$\boldsymbol{U}_d$ [5]	$\boldsymbol{U}_d$ [12]	$\boldsymbol{U}_d$ [6]	$\boldsymbol{U}_d$ [13]	$\boldsymbol{U}_d$ [7]	$\boldsymbol{U}_d$ [14]
	−2	$\boldsymbol{U}_d$ [26]	$\boldsymbol{U}_d$ [20]	$\boldsymbol{U}_d$ [21]	$\boldsymbol{U}_d$ [15]	$\boldsymbol{U}_d$ [22]	$\boldsymbol{U}_d$ [16]	$\boldsymbol{U}_d$ [23]	$\boldsymbol{U}_d$ [17]	$\boldsymbol{U}_d$ [24]	$\boldsymbol{U}_d$ [18]	$\boldsymbol{U}_d$ [25]	$\boldsymbol{U}_d$ [19]
2	2	$\boldsymbol{U}_d$ [23]	$\boldsymbol{U}_d$ [17]	$\boldsymbol{U}_d$ [24]	$\boldsymbol{U}_d$ [18]	$\boldsymbol{U}_d$ [25]	$\boldsymbol{U}_d$ [19]	$\boldsymbol{U}_d$ [26]	$\boldsymbol{U}_d$ [20]	$\boldsymbol{U}_d$ [21]	$\boldsymbol{U}_d$ [15]	$\boldsymbol{U}_d$ [22]	$\boldsymbol{U}_d$ [16]
	1	$\boldsymbol{U}_d$ [5]	$\boldsymbol{U}_d$ [12]	$\boldsymbol{U}_d$ [6]	$\boldsymbol{U}_d$ [13]	$\boldsymbol{U}_d$ [7]	$\boldsymbol{U}_d$ [14]	$\boldsymbol{U}_d$ [8]	$\boldsymbol{U}_d$ [9]	$\boldsymbol{U}_d$ [3]	$\boldsymbol{U}_d$ [10]	$\boldsymbol{U}_d$ [4]	$\boldsymbol{U}_d$ [11]
	0	$\boldsymbol{U}_d$ [0]	$\boldsymbol{U}_d$ [2]	$\boldsymbol{U}_d$ [1]	$\boldsymbol{U}_d$ [1]	$\boldsymbol{U}_d$ [0]	$\boldsymbol{U}_d$ [2]	$\boldsymbol{U}_d$ [1]	$\boldsymbol{U}_d$ [1]	$\boldsymbol{U}_d$ [0]	$\boldsymbol{U}_d$ [2]	$\boldsymbol{U}_d$ [1]	$\boldsymbol{U}_d$ [1]
	−1	$\boldsymbol{U}_d$ [7]	$\boldsymbol{U}_d$ [14]	$\boldsymbol{U}_d$ [8]	$\boldsymbol{U}_d$ [9]	$\boldsymbol{U}_d$ [3]	$\boldsymbol{U}_d$ [10]	$\boldsymbol{U}_d$ [4]	$\boldsymbol{U}_d$ [11]	$\boldsymbol{U}_d$ [5]	$\boldsymbol{U}_d$ [12]	$\boldsymbol{U}_d$ [6]	$\boldsymbol{U}_d$ [13]
	−2	$\boldsymbol{U}_d$ [19]	$\boldsymbol{U}_d$ [26]	$\boldsymbol{U}_d$ [20]	$\boldsymbol{U}_d$ [21]	$\boldsymbol{U}_d$ [15]	$\boldsymbol{U}_d$ [22]	$\boldsymbol{U}_d$ [16]	$\boldsymbol{U}_d$ [23]	$\boldsymbol{U}_d$ [17]	$\boldsymbol{U}_d$ [24]	$\boldsymbol{U}_d$ [18]	$\boldsymbol{U}_d$ [25]

The DTC standard method for the three-level inverter can be improved in two ways. The first way is to change the entries in vector selection table, but this will cause an increase of torque ripples [5]. The other (better) method consists in the modification of the control system by taking into account the angle δ (6) described as a deviation of the U_s^* stator voltage vector from the q-axis of the dq reference frame [4, 5].

$$\delta = arctg\frac{-U_{sd}^*}{U_{sq}^*} = \frac{-(R_s i_{sd}^* - \omega_s L_{\sigma s} i_{sq}^*)}{E + R_s i_{sq}^* + \omega_s L_{\sigma s} i_{sd}^*}. \tag{6}$$

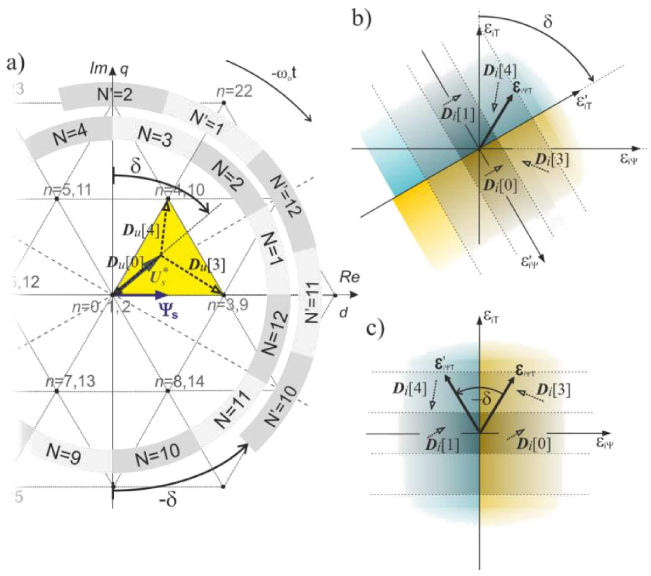

Fig. 7. The principle of sectors boundaries shifting (a) as well as the rotation of error comparator boundaries and its (b) equivalent operation made on the error vector (c)

The δ angle should be taken into account in two parts of the control system i.e. in sector selection and error vector calculation. The principle of determining new N' sector boundaries is based on the rotation of original sector boundaries by $-\delta$ angle, as is shown in Fig. 7a. Having done this it is possible to select from the vector selection table a group of vectors which allows for an appropriate control of current at any instant of time. The above operation proves difficult and time consuming. However, the same faster results can be achieved by selecting a N sector, which is based on summated the $\varphi_{\Psi s}$ stator flux angle and the δ angle according to the schematic diagram of the DTC-sδ-12s method. Appropriate flux and torque control in the control system with rotated sector boundaries requires additional modification of the torque and flux control circuit i.e. the rotation of error comparator boundaries by δ angle (Fig. 7b). But, as in the situation described above, the operation is difficult and time consuming and could be replaced by an equivalent operation i.e. the rotation of an error vector by $-\delta$ angle (Fig. 7c) (7).

Since the change of the values of error vector components is only possible on the same scale [4], the operation of error vector rotation (7) requires rescaling torque and flux errors to the current scale (5).

$$\varepsilon'_{i\Psi T} = \varepsilon_{i\Psi T} e^{-j\delta}. \tag{7}$$

Schematic diagram of the DTC-s δ-12s with the three-level inverter is shown in Fig. 8.

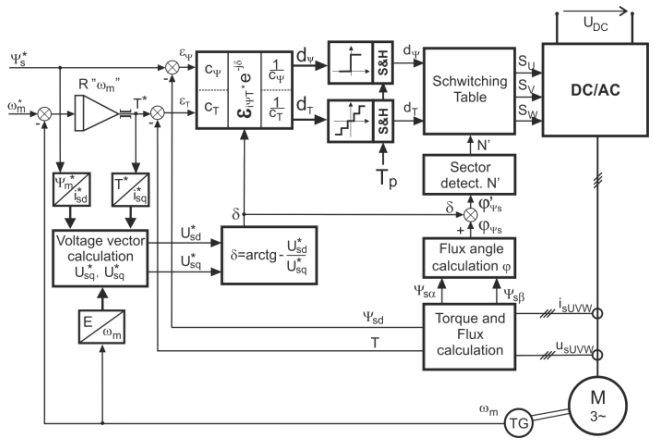

Fig. 8. Schematic diagram of the DTC-s δ-12s method

4.2. DTFC-3L-3Am method. The DTFC-3L-3Am method, similarly to the standard DTC method, makes use of 6 sector area division of inverter output voltage vectors (Fig. 5a), but in order to take full advantage of the three-level inverter each of the sectors is divided into four equilateral triangles (Fig. 9a) [13]. This division allows to choose a triangle in which the U_s^* stator voltage vector is currently located.

Thanks to this, torque and flux can be controlled by inverter output voltage vectors that give the shortest current derivatives D_i [n] (4) which in turn increase control quality and decrease switching frequency.

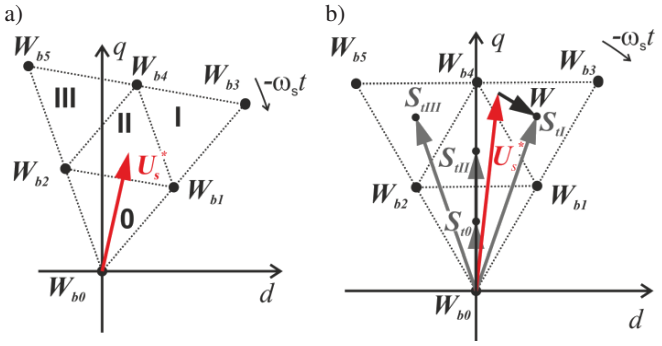

Fig. 9. Area division of inverter output voltage vectors in each sector into four equilateral triangles for the DTFC-3L-3Am method (a) as well as graphic representation of W and S_t center of triangle vectors

Vectors U_{sec1} and U_{sec2} (Fig. 10) are introduced in order to choose a suitable triangle where the U_s^* stator voltage vector is currently located. These variables are defined by Eqs. (8) and (9) [13].

$$\mathbf{U}_{\mathrm{sec}\,1} = \mathbf{W}_{b4} = |\mathbf{U}_{\mathrm{sec}\,1}| \cdot e^{j\varphi_{\mathbf{U}_{\mathrm{sec}\,1}}}, \tag{8}$$

$$\mathbf{U}_{\mathrm{sec}\,2} = \mathbf{U}_s^* - \mathbf{U}_{\mathrm{sec}\,1} = |\mathbf{U}_{\mathrm{sec}\,2}| \cdot e^{j\varphi_{\mathbf{U}_{\mathrm{sec}\,2}}}, \tag{9}$$

$$\varphi\varphi_{U_{\mathrm{sec}\,2}} = arcsin\left(\frac{|\mathbf{U}_s^*|}{|\mathbf{U}_{\mathrm{sec}\,1} - \mathbf{U}_s^*|} sin\left(\varphi\varphi_{U_{sec1}} - \varphi\varphi_{\mathbf{U}_s^*}\right)\right). \tag{9a}$$

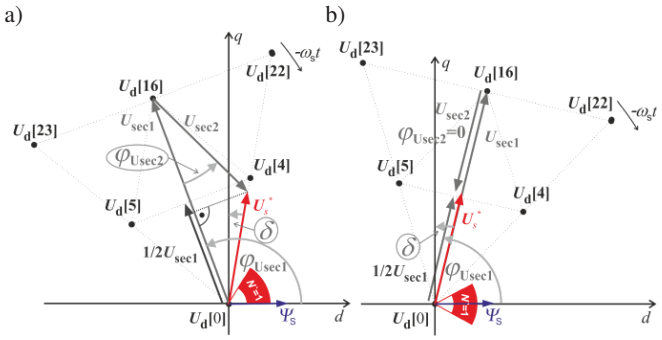

Fig. 10. Graphic interpretation of the U_{sec1}, and U_{sec2}voltage vectors, as well as angleϕ_{Usec2} for both situations i.e. when flux vector is in the beginning (a) and in the middle (b) of sector N=1

If the projection of the U_s^* stator voltage vector on the U_{sec1} vector is shorter than half of vector's U_{sec1} length, then the U_s^* vector is located inside triangle 0. This condition is described by inequality (10).

$$\left|\frac{\mathbf{U}_{\mathrm{sec}\,1}}{2}\right| > Re\left\{|\mathbf{U}_s^*|\, e^{j(\varphi_{U_{sec1}} - \varphi_{\mathbf{U}_s^*})}\right\}. \tag{10}$$

In the case when inequality (10) is unfulfilled, the choice of a triangle is dependent on the ϕ_{Usec2} angle, according to Table 2.

Table 2
Triangle selection table

$\varphi\varphi_{U\,\mathrm{sec}\,2} \in (\pi/6, \pi/2)$	triangle I
$\varphi\varphi_{U\,\mathrm{sec}\,2} \in (-\pi/6, \pi/6)$	triangle II
$\varphi\varphi_{U\,\mathrm{sec}\,2} \in (-\pi/2, -\pi/6)$	triangle III

In the DTFC-3L-3Am method error distribution areas for each of the equilateral triangles are determined in the way shown in Fig. 11 [13].

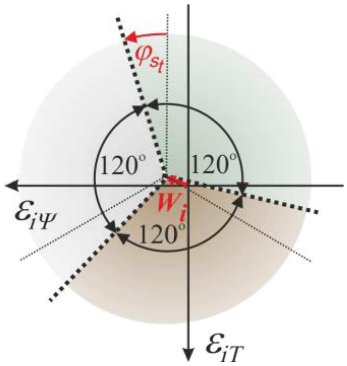

Fig. 11. Graphic representation of the error distribution area for each triangle in the DTFC-3L-3Am method

The boundaries of the error distribution area in the DTFC-3L-3Am method are made up of three half-lines of common origin and they are turned against each other by 120°. These boundaries are shifted by the angle ϕ_S (S_t vector angle) with respect to the q-axis and the common origin of the boundaries is shifted from the origin of the coordinate system by the W_i vector (Fig. 11).

The W_i vector (11) is proportional to the voltage vector W (12) that constitutes the difference between the S_t vector (the center of delta composed of three voltage vectors) and the U_s^* stator voltage vector (Fig. 9b). The vector S_t is dependent on the triangle where the U_s^* stator voltage vector is currently located. The vector is described by formula (13).

$$\mathbf{W}_i = \frac{\mathbf{W}}{L_{\sigma s}} T_p, \tag{11}$$

where T_p – sampling time.

The W vector is calculated using the formula (12) as shown in Fig. 9.

$$\mathbf{W} = \mathbf{S}_t - \mathbf{U}_s^*, \tag{12}$$

$$\mathbf{S_t} = |\mathbf{S_t}| \cdot e^{j\varphi_{\mathbf{St}}} = \begin{cases} \frac{1}{3}(\mathbf{W}_{b0} + \mathbf{W}_{b1} + \mathbf{W}_{b2}), \\ \qquad \text{for triangle 0} \\ \frac{1}{3}(\mathbf{W}_{b1} + \mathbf{W}_{b3} + \mathbf{W}_{b4}), \\ \qquad \text{for triangle I} \\ \frac{1}{3}(\mathbf{W}_{b1} + \mathbf{W}_{b2} + \mathbf{W}_{b4}), \\ \qquad \text{for triangle II} \\ \frac{1}{3}(\mathbf{W}_{b2} + \mathbf{W}_{b4} + \mathbf{W}_{b5}), \\ \qquad \text{for triangle III} \end{cases} \tag{13}$$

Table 3
Vector selection table for the DTFC-3L-3Am method

$\varphi_{\varepsilon''_{i\Psi M}}$	Triangle	$N=1$	$N=2$	$N=3$	$N=4$	$N=5$	$N=6$
		inverter voltage vectors					
$\left(\frac{-\pi}{6}, \frac{\pi}{2}\right)$	0	U_d [4] U_d [10]	U_d [5] U_d [11]	U_d [6] U_d [12]	U_d [7] U_d [13]	U_d [8] U_d [14]	U_d [3] U_d [15]
	I	U_d [22]	U_d [23]	U_d [24]	U_d [25]	U_d [26]	U_d [21]
	II	U_d [4] U_d [10]	U_d [5] U_d [11]	U_d [6] U_d [12]	U_d [7] U_d [13]	U_d [8] U_d [14]	U_d [3] U_d [9]
	III	U_d [16]	U_d [17]	U_d [18]	U_d [19]	U_d [19]	U_d [15]
$\left(\frac{-5\pi}{6}; \frac{-\pi}{6}\right)$	0	U_d [0]	U_d [1]	U_d [2]	U_d [0]	U_d [1]	U_d [2]
	I	U_d [4] U_d [10]	U_d [5] U_d [11]	U_d [6] U_d [12]	U_d [7] U_d [13]	U_d [8] U_d [14]	U_d [3] U_d [9]
	II	U_d [16]	U_d [17]	U_d [18]	U_d [19]	U_d [19]	U_d [15]
	III	U_d [5] U_d [11]	U_d [6] U_d [12]	U_d [7] U_d [13]	U_d [8] U_d [14]	U_d [3] U_d [9]	U_d [4] U_d [10]
$\left(\frac{\pi}{2}, \frac{7\pi}{6}\right)$	0	U_d [5] U_d [11]	U_d [6] U_d [12]	U_d [7] U_d [13]	U_d [8] U_d [14]	U_d [3] U_d [9]	U_d [4] U_d [10]
	I	U_d [16]	U_d [17]	U_d [18]	U_d [19]	U_d [19]	U_d [15]
	II	U_d [5] U_d [11]	U_d [6] U_d [12]	U_d [7] U_d [13]	U_d [8] U_d [14]	U_d [3] U_d [9]	U_d [4] U_d [10]
	III	U_d [23]	U_d [24]	U_d [25]	U_d [26]	U_d [21]	U_d [22]

where W_{b0}, W_{b1}, W_{b2}, W_{b3}, W_{b4}, W_{b5} – voltage vectors U_d[n] in the dq reference frame for the currently used sector N (Fig. 9).

Ultimately, the DTFC-3L-3Am control system for the three-level inverter takes the form shown in Fig. 12.

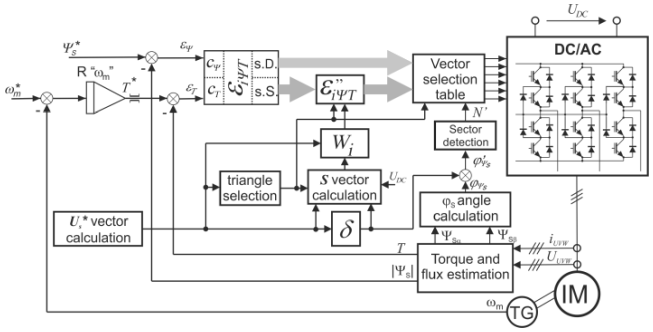

Fig. 12. Schematic diagram of the DTFC-3L-3Am method

In the DTFC-3L-3Am method the real values of torque and flux are compared to corresponding set values. The obtained errors are computed into the current scale in order to create current error vector $\varepsilon_{i\Psi T}$ (5). The error vector $\varepsilon_{i\Psi T}$ is thus subsequently transformed into $\varepsilon''_{i\Psi T}$ in agreement with the formula (14).

$$|\varepsilon''_{i\Psi T}| \cdot e^{j\varphi_{\varepsilon'''_{i\Psi T}}} = \begin{cases} (\varepsilon_{i\Psi} + j\varepsilon_{iT} - \mathbf{W}_i) \cdot e^{-j\varphi_{\mathbf{S_t}}}, \\ \text{for triangles 0,I,III} \\ (\varepsilon_{i\Psi} - j\varepsilon_{iT} - \mathbf{W}_i) \cdot e^{-j\varphi_{\mathbf{S_t}}}, \\ \text{for triangle II} \end{cases} \quad (14)$$

The choice of inverter voltage vector from the vector voltage selection table (Table 3) is based on the information about current N sector, the triangle where the U_s^* stator voltage vector is currently located, as well as the angle of the error vector $\varepsilon''_{i\Psi T}$.

5. Comparison of DTFC-3L-3Am and DTC-sδ-12s methods

The investigations were performed for two values of load i.e. 5 N·m and 10 N·m, and for three set values of angular speed i.e. 10 rad/s, 50 rad/s and 80 rad/s. The motor used in the investigations had the following nominal values: $P_n = 4$ kW, $U_n = 400$ V, $f_n = 50$ Hz, $I_n = 8.3$ A, $\omega_n = 150$ rad/s, $\cos\phi_n = 0.82$. The sampling time of the control DC/AC converter amounted to 40 μs.

The basis for comparing the methods were the coefficients described by dependencies (14) and (15) [4] as well as THD value.

$$T_{(puls)RMS} = \sqrt{\frac{1}{T_o}\int_0^{T_o}(T - T_{AV})^2 dt}, \quad (15)$$

where $T_{(plus)RMS}$ – RMS value of all of torque harmonics for constant torque set value, T_0 – period of phase current, T – instantaneous value of electromagnetic torque, T_{AV} – mean value of electromagnetic torque.

$$I_{U(puls)RMS} = \sqrt{\frac{1}{T_o}\int_0^{T_o}(i_U - i_{U1})^2 dt}, \quad (16)$$

where $I_{U(puls)RMS}$ – RMS value of phase current harmonics after subtraction the instantaneous value of the first harmonic, i_U – instantaneous value of phase current, i_{U1} – instantaneous value of the first harmonic of phase current.

Both methods have shown similar, very good performance. The flux in both methods has almost a perfect sinusoidal shape (Fig. 13ab). The switching frequencies in nearly the whole control range are approximately the same. The greatest differences can be seen for 10 rad/s of angular speed and 10 N·m of load. In this case the switching frequency for the DTFC-3L-3Am is 10% lower than for the DTC-sδ-12s method.

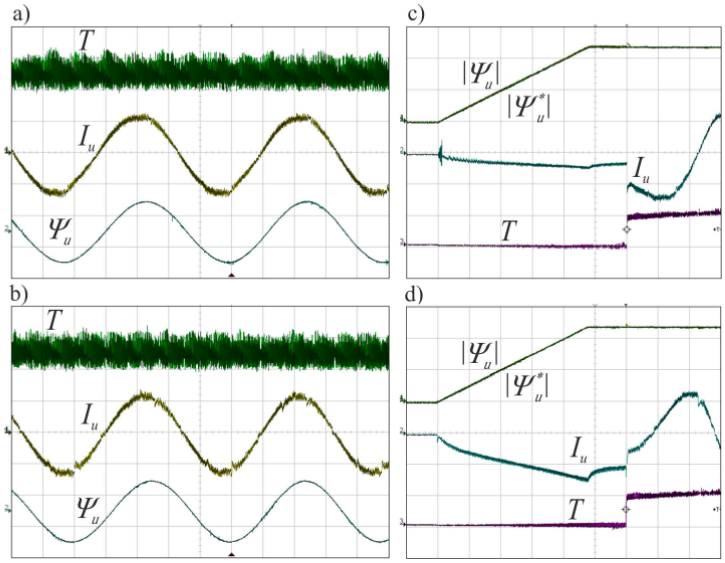

Fig. 13. Time courses of torque, stator phase current and stator phase flux for 10 rad/s angular speed and 5 N·m load for DTFC-3L-3Am (a) and DTC-sδ-12s (b) methods (time [50 ms/div], I_u [5 A/div], Ψ_u[1 Wb/div], T [2 N·m/div])) as well as time courses of set and real stator flux absolute values, phase current and torque during startup for DTFC-3L-3Am (c) and DTC-sδ-12s (d) methods (time [50 ms/div], I_u [5 A/div], Ψ_u [0.4 Wb/div], T [10 N·m/div])

Table 4
Comparison of DTC-sδ-12s and DTFC-3L-3Am methods in static state

Method	Set values							
	ω_m^*	rad/s	10		50		80	
	T	N·m	5	10	5	10	5	10
DTFC-3L-3Am	$I_{(puls)RMS}$	A	0.258	0.279	0.290	0.269	0.263	0.276
DTC-sδ-12s			0.309	0.319	0.313	0.298	0.285	0.312
DTFC-3L-3Am	$T_{(puls)RMS}$	N·m	0.491	0.457	0.590	0.548	0.443	0.511
DTC-sδ-12s			0.516	0.513	0.592	0.574	0.470	0.571
DTFC-3L-3Am	*THD*	–	0.056	0.053	0.062	0.050	0.056	0.051
DTC-sδ-12s		–	0.067	0.060	0.067	0.056	0.061	0.057
DTFC-3L-3Am	f	kHz	0.88	0.63	3.24	3.17	3.39	3.56
DTC-sδ-12s			0.88	0.70	3.25	3.14	3.52	3.54

The use of the DTFC-3L-3Am method reduces coefficient values of torque deformations up to 11% compared with the DTC-sδ-12s method.

The use of the DTFC-3L-3Am method reduces coefficient values of current deformations by approximately 7–17% and THD by approximately 7–15% compared with the DTC-sδ-12s method.

Both methods make it possible to generate nominal flux for a set zero angular speed with a very good accuracy. As it can be seen in Fig. 13cd the real value of a flux almost fully covers its set value. The above is desirable in order to achieve better performance at the startup. As in the case shown in Fig. 13cd when torque is not set until a flux has achieved its nominal value by a linear increase, large ripples of current during a startup are eliminated.

6. Conclusions

The investigation results have shown that the two methods presented above are characterized by a very good performance. The switching frequencies almost within the whole range of control are low and very similar, which means that they have a very good efficiency. The DTFC-3L-3Am method shows lower values of current and torque distortion coefficients as well as lower THD value. The differences in the control quality are greater for higher values of torque.

Both methods allow to achieve the nominal flux at the zero angular speed. It is very helpful in the case if fine performances during startup of an induction machine are desirable.

It should be emphasized that the DTC-sδ-12s method is much more similar to the standard DTC method and thus easier to implement it in control systems.

Acknowledgements. The work was supported by funds for the scientific project S/WE/3/2013.

REFERENCES

[1] M. Korzeniewski and A. Sikorski, "Three-level DC/AC inverter controlled by direct torque and flux control method of induction motor", *Electrical Review* 86, 263–268 (2010).

[2] I. Takahashi and T. Noguchi, "A new quick – response and high – efficiency control strategy of an induction motor", *IEEE Trans. on Ind. Appl.* 22, 820–827 (1986).

[3] G.S. Buja and M.P. Kazmierkowski, "Direct torque control of PWM inverter-fed AC motors-a survey", *IEEE Trans. on Ind. Electronics* 51 (4), 744–757 (2004).

[4] A. Sikorski, *Direct Torque and Flux Regulation of an Induction Motor,* Białystok Technical University, Białystok, 2009, (in Polish).

[5] A. Sikorski, M. Korzeniewski, A. Ruszczyk, M.P. Kaźmierkowski, P. Antoniewicz, W. Kolomyjski, and M. Jasiński, "A comparison of properties of direct torque and flux control methods (DTC-SVM,DTC-δ, DTC-2x2, DTFC-3A)", *Int. Conf. on Computer as a Tool EUROCON 2007* 1, 1733–1739 (2007).

[6] R. Grodzki, "Nowy algorytm bezpośredniej regulacji momentu i strumienia maszyny indukcyjne", *Electrical Review* 88 (12), 34–37 (2012).

[7] M.P. Kazmierkowski and A.B. Kasprowicz, "Improved direct torque and flux vector control of PWM inverter-fed induction motor drives", *IEEE Trans. on Ind. Electronics* 42 (4), 344–350 (1995).

[8] V. Ambrozic, G.S. Buja, and R. Menis, "Band-constrained technique for direct torque control of induction motor", *IEEE Trans. on Ind. Electronics* 51 (4), 776–784 (2004).

[9] P. Wójcik, D. Świerczynski, M. P. Kazmierkowski, and M. Janaszek, "Direct torque and flux control of PWM inverter fed induction motor drive for electrical tram transportation", *Electrical Review* 84 (12), 115–118 (2008).

[10] H. Abu-Rub, D. Stando, and M.P. Kaźmierkowski, "Simple speed sensorless DTC-SVM scheme for induction motor drives", *Bull. Pol. Ac.: Tech.* 61 (2), 301-307 (2013).

[11] C. Lascu, I. Boldea, and F. Blaabjerg, "Variable structure direct torque control – a class of fast and robust controllers for induction machine drives", *IEEE Trans. on Ind. Electronics* 51 (4), 785–792 (2004).

[12] S. Styński, M.P. Kaźmierkowski, and D. Świerczynski, "Analysis of the multistage AC/DC/AC convertor with capacitors with variable voltage powered by the single phase source", *Electrical Review* 87 (1), 153–158 (2011), (in Polish).

[13] K. Kulikowski and A. Sikorski, "Efficiency improvement due to direct torque and flux three levels three areas control method applied to small hydroelectric power plant", *Bull. Pol. Ac.: Tech.* 59 (4), 569–574 (2011).